



Thermodynamically consistent modeling of gas flow and adsorption in porous media

Magnus Aa. Gjennestad^{a,*}, Øivind Wilhelmsen^{a,b}

^a SINTEF Energy Research, PO Box 4761 Torgarden, NO-7465 Trondheim, Norway

^b PoreLab, Department of Chemistry, Norwegian University of Science and Technology, NO-7491 Trondheim, Norway

ARTICLE INFO

Keywords:

Porous media
Thermodynamics
Heat transport
Adsorption
Entropy production

ABSTRACT

In modeling of gas flow through porous media with adsorption, the thermodynamic properties of the adsorbed phase are usually approximated by those of the bulk liquid. Using non-isothermal, gaseous transport of moist air through a porous insulation material as example, we show that this leads to violation of the second law of thermodynamics and a negative entropy production. To resolve this violation, we use information about the adsorption and thermodynamic properties of bulk fluids to derive consistent thermodynamic properties of the adsorbed phase, such as the chemical potential, enthalpy and entropy. The resulting chemical potential of the adsorbed phase is a starting point for rate-based models for adsorption based on non-equilibrium thermodynamics. Incorporating the consistent thermodynamic description into the energy, entropy and momentum balances restores agreement with the second law of thermodynamics. We show that the temperature evolution in the porous medium from the consistent description differs from the standard formulation only if the adsorption depends explicitly on temperature. This highlights the importance of characterizing the temperature dependence of the adsorption with experiments or molecular simulations for accurate non-isothermal modeling of porous media.

1. Introduction

Due to the high surface to volume ratio of porous materials, the amount of matter that can be adsorbed onto and into the porous structure may be large and strongly influence behavior [1–3]. This makes porous materials like zeolites and metal organic frameworks candidates to store hydrogen [4–6] or to capture CO₂ and methane [7–9]. Both pressure and temperature swing adsorption are promising technologies to capture CO₂ from power and industrial flue gases, as well as to remove green house gases from air to deliver negative emissions [10]. A challenge common to both of these examples is the necessity to effectively manage and reduce the heat involved in the adsorption process [11–13].

The heat of sorption is of importance to a wide variety of processes and phenomena. It is necessary to account for this property to arrive at a reliable description of the temperature evolution in insulation materials for buildings [14–17]. In drying of paper, the duration of the process is intimately related to the heat of sorption [18–20]. This is also the case

for other drying processes, such as drying of soil in agriculture [21,22], of pharmaceutical materials or food [23–25], paint [26,27] or coal [28].

Non-isothermal modeling of fluid flow through porous media has been an important tool in the study of the examples mentioned above and many other that involve adsorbed fluid phases [18,24,27]. In many of these examples, only one component adsorbs onto and into the porous structure. For instance, the water adsorbed in insulation materials is assumed to be pure, since the solubility of the components of air such as nitrogen and oxygen is very low. Furthermore, the properties of the adsorbed phase can be difficult to measure directly. A common approach is therefore to approximate the thermodynamic properties of the adsorbed phase with those of the bulk phase [15,22,29]. This is a common, yet questionable approximation that is frequently used in non-isothermal modeling of porous media [14,15,30,31]. In this work, we present an in-depth and critical assessment of this approach. By deriving the entropy production of transient, non-isothermal flow through porous media and performing numerical simulations, we show that if the properties of the adsorbed phase are taken to be the same as those of the bulk liquid phase, the entropy balance is not satisfied, and the

* Corresponding author.

E-mail address: magnus.gjennestad@sintef.no (M.Aa. Gjennestad).

second law of thermodynamics is violated. This demonstrates that the entropy balance is an invaluable tool in evaluating the consistency in modeling of flow through porous media [32–37].

To remedy the violation of the second law of thermodynamics, we derive a consistent thermodynamic framework for single-component adsorbed phases in contact with ideal gases, which is based on a work by T. Hill from 1949 [38]. The advantage of the derived framework is that it is self-consistent with the model or data used for the sorption isotherm and the thermodynamic properties of the bulk fluids. By combining this framework with the balance equations for energy, entropy and momentum in the porous medium, we show that the entropy balance for the consistent description is satisfied, and in agreement with the second law of thermodynamics [39]. Using non-isothermal, gaseous transport of moist air through a porous insulation material as example [16], we show that the temperature evolution in the porous medium from the consistent description differs from the standard formulation only if the adsorption depends explicitly on temperature. This highlights the importance of characterizing the temperature dependence of the adsorption by use of experiments or molecular simulations [40–42] for accurate non-isothermal modeling of porous media.

There are several reasons to use a thermodynamically consistent description of the adsorbed phase. For instance, sorption in porous media has shown to exhibit an intriguing behavior, where slow and fast sorption sites simultaneously influence the kinetics [43–47]. Kohler et al. presented the parallel exponential kinetics model to describe this phenomenon [45,46]. In their work, they state that the chemical potential difference between the vapor phase and the adsorbed phase is the true driving force of mass transfer. However, since the chemical potential of the adsorbed phase has been inaccessible, a difference in adsorbed mass has been used as an alternative driving force [43–47]. This has led to sample-specific models of the adsorption kinetics, with limited predictive ability. The thermodynamic model for the adsorbed phase presented in this work establishes the foundation for developing more sophisticated sorption kinetics models that are based on non-equilibrium thermodynamics [48]. A consistent description of the adsorbed phase is also a prerequisite for analysis of thermodynamic stability heterogeneous microstructures such as adsorbed films and droplets in porous media [49].

The article will be structured as follows. We present first a consistent thermodynamic description of adsorbed phases in Sec. 2. The transport equations are presented Sec. 3, where they are combined with the entropy balance and the Gibbs relation to derive the entropy production. Next, two cases studied using numerical simulations are described in Sec. 4 and results are discussed in detail in Sec. 5. Concluding remarks are provided in Sec. 6.

2. Thermodynamics of adsorbed phases

In this section, we derive a consistent thermodynamic description of a single-component adsorbed phase based on a work by T. Hill from 1949 [38]. The thermodynamic description takes the form of a fundamental relation for the adsorbed phase, from which other thermodynamic properties, such as chemical potential, density, enthalpy and entropy, can be derived by differentiation.

A common procedure in modeling of transport through porous media is to assume that the thermodynamic properties of the adsorbed phase are the same as those of a pure, bulk liquid at ambient conditions. We will show in Sec. 5 that following this approach can lead to violation of the second law of thermodynamics. Further details on the thermodynamic description of the bulk liquid used here can be found in the Supplementary Information (SI).

2.1. Consistent thermodynamic properties of the adsorbed phase

We will now derive a thermodynamic framework to describe the adsorbed phase by following Hill [38]. In this description, the adsorbed

phase (a) is, in general, different from a bulk liquid (ℓ) or a bulk gas phase (g). The total internal energy is $U^a(S^a, V^a, A, N^a)$ and its differential is

$$dU^a = TdS^a - p dV^a - \varphi dA + \mu^a dN^a. \quad (1)$$

Herein, T is the temperature, S^a is the entropy, p is the pressure, V^a is the volume and N^a is the number of particles in the adsorbed phase. In addition, A is the area of adsorbent covered by the adsorbed phase and φ is the *spreading pressure*. The latter is equal to $\gamma^0 - \gamma^a$ where γ^0 is the surface tension of the clean adsorbent and γ^a is the surface tension of the adsorbent with the adsorbed phase on it.

The Euler equation for the adsorbed phase is [38]

$$U^a = T S^a - p V^a - \varphi A + \mu^a N^a. \quad (2)$$

The Helmholtz energy, the Gibbs energy and enthalpy follow from the definitions that can be found in [38]. The definition of the enthalpy is $H^a = U^a + p V^a + \varphi A$ and the Gibbs–Duhem equation for the adsorbed phase is

$$N^a d\mu^a = -S^a dT + V^a dp + A d\varphi. \quad (3)$$

As a *new* thermodynamic potential in addition to those defined in [38], we will use $X^a = U^a - T S^a + p V^a$. This will be useful when deriving a fundamental relation for the adsorbed phase. Through Eq. (2) the potential X^a may also be expressed as

$$X^a = -\varphi A + \mu^a N^a. \quad (4)$$

Its differential is

$$dX^a = -S^a dT + V^a dp - \varphi dA + \mu^a dN^a, \quad (5)$$

and its canonical variables are T , p , A and N^a . The potential X^a is first-order homogeneous in A and N^a , so that

$$\lambda X^a(T, p, A, N^a) = X^a(T, p, \lambda A, \lambda N^a). \quad (6)$$

Setting $\lambda = 1/N^a$ yields the molar potential x^a ,

$$X^a(T, p, A, N^a) / N^a = X^a(T, p, A/N^a, 1) = x^a(T, p, \Gamma), \quad (7)$$

where $\Gamma = N^a/A$ is the adsorption. Using Eq. (4), we get

$$x^a = \mu^a - \varphi / \Gamma. \quad (8)$$

The differential of x^a is

$$dx^a = -s^a dT + v^a dp + \{\varphi / \Gamma^2\} d\Gamma, \quad (9)$$

where s^a is the molar entropy and v^a is the molar volume.

2.1.1. Calculating the spreading pressure from the adsorption

In this section, we will present a procedure for obtaining the spreading pressure φ by integration of an empirical model for the adsorption from a gas mixture. We assume that the adsorbed phase is pure, but that the gas it adsorbs from is a mixture of M components. The adsorbing component is Component 1 in the gas phase. Chemical equilibrium between the adsorbed phase and the gas then implies that $\mu^a(T, p, \Gamma) = \mu_1^g(T, p, \mathbf{z}^g)$, where \mathbf{z}^g are the component mole fractions in the gas. Bold symbols are used to indicate vector quantities. This equation defines the equilibrium adsorption $\Gamma(T, p, \mathbf{z}^g)$. We will here consider the less general form $\Gamma(\hat{p}_1, T)$ because it is commonly used in the literature [16]. The quantity \hat{p}_1 is the dimensionless partial pressure of the adsorbing component,

$$\hat{p}_1 = \frac{z_1^g p}{p_1^{\text{sat}}(T)}, \quad (10)$$

where $p_1^{\text{sat}}(T)$ is the saturation pressure and thus $\hat{p}_1 = 1$ at saturation. For water in air, \hat{p}_1 is the same as relative humidity.

The chemical potential of Component 1 in the gas phase can, in general, be written as [50, pp. 34-37]

$$\mu_1^g(T, p, z^g) = \mu_1^i(T, p^\circ) + RT \log \left(\frac{\zeta_1^g(T, p, z^g) p z_1^g}{p^\circ} \right), \quad (11)$$

where R is the universal gas constant, $\mu_1^i(T, p^\circ)$ is the ideal gas chemical potential evaluated at the reference pressure p° and ζ_1^g is the fugacity coefficient. The differential of μ_1^g , assuming constant T and p and using that $dz_M^g = \sum_{i=1}^{M-1} dz_i^g$, is

$$d\mu_1^g = \frac{RT}{z_1^g} dz_1^g + \frac{RT}{\zeta_1^g} \sum_{i=1}^{M-1} \left\{ \left(\frac{\partial \zeta_1^g}{\partial z_i^g} \right)_{T, p, z_{k \neq i}^g} - \left(\frac{\partial \zeta_1^g}{\partial z_M^g} \right)_{T, p, z_{k \neq M}^g} \right\} dz_i^g. \quad (12)$$

Dividing the Gibbs–Duhem equation (3) by A , and assuming constant T and p , gives

$$d\varphi = \Gamma d\mu^a. \quad (13)$$

We may now obtain the spreading pressure by integrating Eq. (13). During the integration, we let T and p be constant and assume equilibrium between the gas and the adsorbed phase, so that $d\mu^a = d\mu_1^g$. Furthermore, we let the change in z_M^g be such that only dz_1^g in Eq. (12) is not zero. The integration path starts at $z_1^g = 0$, where there is no adsorption, and the adsorption commences by increasing the mole fraction of Component 1 in the gas phase to z_1^g . Since φ should be zero, i.e. $\gamma^a = \gamma^0$, when $z_1^g = 0$ and there is no adsorption [51], the integral of Eq. (13) becomes

$$\varphi = RT \int_0^{z_1^g} \Gamma \left\{ \frac{1}{z_1^g} + \frac{1}{\zeta_1^g} \left(\frac{\partial \zeta_1^g}{\partial z_1^g} \right)_{T, p, z_{k \neq 1}^g} - \frac{1}{\zeta_1^g} \left(\frac{\partial \zeta_1^g}{\partial z_M^g} \right)_{T, p, z_{k \neq M}^g} \right\} dz_1^g. \quad (14)$$

Adsorption models are often functions of the partial pressure. For simplicity, we will from here on assume that the gas phase is ideal. At constant temperature and pressure, the differential of the dimensionless partial pressure is

$$d\hat{p}_1 = \frac{p}{p_1^{\text{sat}}(T)} dz_1^g. \quad (15)$$

Hence, for an ideal gas Eq. (14) reduces to

$$\varphi(\hat{p}_1, T) = RT \int_0^{\hat{p}_1} \frac{\Gamma}{\hat{p}_1} d\hat{p}_1. \quad (16)$$

We can thus obtain the spreading pressure from an integral of the adsorption $\Gamma(\hat{p}_1, T)$.

In the fundamental relation, which we derive in the next section, we express φ as a function of parameters of the adsorbed phase only. We accomplish this by assuming that $\Gamma(\hat{p}_1, T)$ is a strictly increasing function of \hat{p}_1 for every value of T . The function $\Gamma(\hat{p}_1, T)$ is then invertible and the function $\hat{p}_1(\Gamma, T)$ exists. In the next section we will therefore treat φ as a function of Γ and T with the understanding that this is accomplished by combining $\hat{p}_1(\Gamma, T)$ and Eq. (16), which yields the function $\varphi(\Gamma, T) = \varphi(\hat{p}_1(\Gamma, T), T)$. To ease notation, we define

$$\varphi_T = \left(\frac{\partial \varphi}{\partial T} \right)_{\hat{p}_1} = R \int_0^{\hat{p}_1} \frac{1}{\hat{p}_1} \left(\frac{\partial \Gamma}{\partial T} \right)_{\hat{p}_1} d\hat{p}_1, \quad (17)$$

where $\varphi_T = 0$ unless Γ has an explicit dependence on temperature. We refer to functions Γ that depend only on \hat{p}_1 as temperature independent.

2.1.2. A fundamental relation for the adsorbed phase

In this section, we will derive a fundamental relation for the adsorbed phase. Such a relation is a mathematical expression for a thermodynamic potential in terms of its canonical variables [52]. With this in place, other thermodynamic properties can be obtained by differentiation.

To construct the fundamental relation, we use as starting point a thick bulk liquid phase residing on the adsorbent. The liquid phase then desorbs at constant T and p by reducing \hat{p}_1 , i.e. by reducing the mole fraction of the adsorbing component in the gas phase. The initial state is Γ_∞ , corresponding to $\hat{p}_1 = 1$ where the adsorbed phase behaves like a bulk liquid. The resulting potential is found by integrating from Γ_∞ to Γ :

$$x^a(T, p, \Gamma) = x^a(T, p, \Gamma_\infty) + \int_{\Gamma_\infty}^{\Gamma} \left(\frac{\partial x^a}{\partial \Gamma} \right)_{T, p} d\Gamma, \quad (18)$$

$$= \mu^\ell(T, p) - \frac{\gamma^0 - \gamma^\ell}{\Gamma_\infty} + \int_{\Gamma_\infty}^{\Gamma} \frac{\varphi}{\Gamma^2} d\Gamma. \quad (19)$$

We have here used Eq. (8) and that, when $\Gamma = \Gamma_\infty$, then $\hat{p}_1 = 1$, $\mu^a = \mu^\ell$ and $\varphi = \gamma^0 - \gamma^\ell$, where γ^ℓ is the surface tension of the adsorbate surface with a bulk liquid on top. Applying integration by parts,

$$x^a(T, p, \Gamma) = \mu^\ell(T, p) - \frac{\varphi(\Gamma, T)}{\Gamma} + RT \log(\hat{p}_1(\Gamma, T)), \quad (20)$$

and, multiplying with N^a , we arrive at the fundamental relation of the adsorbed phase,

$$X^a(T, p, N^a, A) = N^a \{ \mu^\ell(T, p) - A\varphi(N^a/A, T) / N^a + RT \log(\hat{p}_1(N^a/A, T)) \}. \quad (21)$$

2.1.3. Volume, chemical potential, entropy and enthalpy

From the fundamental relation in Eq. (21) we can derive expressions for the volume, chemical potential, entropy and enthalpy of the adsorbed phase.

The volume is

$$V^a = \left(\frac{\partial X^a}{\partial p} \right)_{T, N^a, A} = N^a \left(\frac{\partial \mu^\ell}{\partial p} \right)_T = N^a v^\ell, \quad (22)$$

with the implication that the density of the adsorbed phase in the consistent thermodynamic description is the same as that of a bulk liquid phase at the same temperature and pressure. The chemical potential is

$$\mu^a = \left(\frac{\partial X^a}{\partial N^a} \right)_{T, p, A} = \mu^\ell + RT \log(\hat{p}_1). \quad (23)$$

Herein, it is the term $RT \log(\hat{p}_1)$ that makes chemical equilibrium possible between the adsorbed phase and Component 1 in the gas phase *away from saturation*.

The entropy of the adsorbed phase is

$$S^a = - \left(\frac{\partial X^a}{\partial T} \right)_{p, A, N^a} = S^\ell - N^a R \log(\hat{p}_1) + \frac{\varphi A}{T} + AT\varphi_T. \quad (24)$$

Here, we have used the triple product rule and the relation [48, pp. 220–221]

$$S^\ell = -N^a \left(\frac{\partial \mu^\ell}{\partial T} \right)_{p, N^a}. \quad (25)$$

From X^a , φ and S^a we may now construct the enthalpy,

$$H^a = H^\ell + \varphi A + AT^2\varphi_T. \quad (26)$$

We have here used that $H^\ell = TS^\ell + \mu^\ell N^a$.

2.1.4. The BET model

To have a concrete example for numerical calculations, we will apply the thermodynamic framework to the well-known Brunauer–Emmett–Teller (BET) adsorption model for single-component adsorption [53,54],

$$\Gamma(\hat{p}, T) = \frac{\alpha^\xi(T) \hat{p}}{\{1 - \hat{p}\} \{1 - \hat{p} + \xi(T) \hat{p}\}}, \quad (27)$$

where

$$\hat{p} = p/p^{\text{sat}}, \quad (28)$$

$$\xi(T) = \frac{j^1}{j^\ell} \exp(\Delta\epsilon/k_B T). \quad (29)$$

Furthermore, $\Delta\epsilon = \epsilon^1 - \epsilon^\ell$, ϵ^1 is the potential energy per molecule in the first adsorbed layer and ϵ^ℓ is the potential energy per molecule in subsequent layers. The ratio j^1/j^ℓ is defined in [54].

We assume that the BET model can be extended to a pure adsorbed phase connected to a multi-component ideal gas phase by replacing p in Eq. (28) with the partial pressure of the adsorbing component in the gas phase. Then $\hat{p} \rightarrow z_1^g p/p_1^{\text{sat}} = \hat{p}_1$, and

$$\Gamma(\hat{p}_1, T) = \frac{\alpha^\xi(T) \hat{p}_1}{\{1 - c\hat{p}_1\} \{1 - \hat{p}_1 + \xi(T) \hat{p}_1\}}. \quad (30)$$

We have here also introduced the constant $c = 1 - \frac{a}{\Gamma_\infty}$, which is smaller than, but very close to 1, and ensures that $\Gamma(\hat{p}_1 = 1, T) = \Gamma_\infty$.

We may now compute the spreading pressure by integrating Eq. (16) with Eq. (30) inserted for Γ . This gives

$$\varphi(\hat{p}_1, T) = RT \frac{\alpha^\xi(T)}{c + \xi(T) - 1} \log\left(\frac{\xi(T) \hat{p}_1 - \hat{p}_1 + 1}{1 - c\hat{p}_1}\right). \quad (31)$$

It is clear that $\varphi = 0$ at $\hat{p}_1 = 0$.

For the cases with water adsorption to be considered in Secs. 4 and 5, the temperature dependence of the adsorption is unknown, as adsorption isotherms are often measured only at a single temperature. To explore the influence of temperature dependence, we linearize $\Gamma(\hat{p}_1, T)$ around the temperature T_0 where the adsorption isotherm is measured. The linearization is a first-order Taylor expansion,

$$\Gamma(\hat{p}_1, T) = \Gamma(\hat{p}_1, T_0) + \{T - T_0\} \left(\frac{\partial \Gamma}{\partial T}\right)_{\hat{p}_1|T_0}, \quad (32)$$

$$= \Gamma(\hat{p}_1, T_0) \left\{1 - \beta \left\{\frac{T}{T_0} - 1\right\}\right\}, \quad (33)$$

where we have defined the dimensionless parameter

$$\beta = -\frac{T_0 \left(\frac{\partial \Gamma}{\partial T}\right)_{\hat{p}_1|T_0}}{\Gamma(\hat{p}_1, T_0)}. \quad (34)$$

In general, β will depend on \hat{p}_1 , but we shall here assume that it is a constant. The spreading pressure is now

$$\varphi(\hat{p}_1, T) = \{T/T_0\} \{1 - \beta \{T/T_0 - 1\}\} \varphi_0(\hat{p}_1), \quad (35)$$

where $\varphi_0(\hat{p}_1) = \varphi(\hat{p}_1, T_0)$.

3. Balance equations for transport

In this section, we formulate balance equations for transport through the pores of a solid matrix (s), where the pore space contains a gas phase (g) and an adsorbed phase (a). These transport equations treat the different phases as interpenetrating continua, i.e. all three phases may be present at any given point in space, and are therefore applicable at length scales much larger than the typical pore size. They are therefore not suitable for resolving transport in individual pores. The transport equations will be formulated on a mass basis and we there-

fore use mass-based quantities for e.g. chemical potential, entropy and internal energy, rather than molar quantities, in this section.

We assume local thermal, chemical and mechanical equilibrium, i.e. that the temperature, pressure and chemical potential of the adsorbing component are locally the same as in the gas phase. The solid is assumed chemically inert and incompressible, so that the solid density ρ^s is constant and known. Also, the porosity ϕ is assumed known. The mass balance for each component i in the gas phase is then

$$\partial_t \{\alpha^g \rho^g w_i^g\} + \nabla \cdot \{\alpha^g \mathbf{j}_i^g\} = \Psi_i^g, \quad (36)$$

where α^g is the volume fraction of the gas phase, w_i^g is the mass fraction of Component i in the gas phase, ρ^g is the mass density of the gas phase and Ψ_i^g accounts for mass exchange with the adsorbed phase. Since we assume that only Component 1 is adsorbed, $\Psi_1^g = -\Psi^a$ and $\Psi_{i \neq 1}^g = 0$.

The flux of Component i through the gas phase is \mathbf{j}_i^g

$$\mathbf{j}_i^g = w_i^g \rho^g \mathbf{v}_i^g = w_i^g \rho^g \mathbf{v}^g + \tilde{\mathbf{j}}_i^g = \tilde{\mathbf{j}}_i^g + \mathbf{j}_i^g, \quad (37)$$

where $\tilde{\mathbf{j}}_i^g$ is the advective part, $\tilde{\mathbf{j}}_i^g$ is the diffusive part, also known as the barycentric mass flux, and $\rho^g \mathbf{v}^g = \sum_{i=1}^M w_i^g \rho^g \mathbf{v}_i^g$. From the definition, $\sum_{i=1}^M \tilde{\mathbf{j}}_i^g = 0$. Summing over all components, the mass balance for the gas phase is

$$\partial_t \{\alpha^g \rho^g\} + \nabla \cdot \{\alpha^g \rho^g \mathbf{v}^g\} = \Psi^g, \quad (38)$$

where $\Psi^g = \sum_{i=1}^M \Psi_i^g$. The mass balance for the adsorbed phase is identical to Eq. (38), with g replaced by a.

The momentum balance of the gas phase is,

$$\partial_t \{\alpha^g \rho^g v_k^g\} + \partial_m \{\alpha^g \rho^g v_k^g v_m^g\} + \alpha^g \partial_k \{p\} = \alpha^g \rho^g g_k + \Theta_k^g + v_k^i \Psi^g, \quad (39)$$

where g_k is the k -component of the gravitational acceleration, Θ_k^g represents the dissipative viscous friction forces acting on the gas in direction k and v_k^i accounts for the momentum transfer associated with mass transfer between the fluid phases. The terms on the right-hand side thus account for, respectively, gravitational forces, friction forces and momentum transfer associated with mass leaving or entering the phase.

The momentum balance of the adsorbed phase is analogous, but contains an additional term proportional to the gradient of the spreading pressure,

$$\begin{aligned} \partial_t \{\alpha^a \rho^a v_k^a\} + \partial_m \{\alpha^a \rho^a v_k^a v_m^a\} + \alpha^a \partial_k \{p\} + \alpha^s \partial_k \{\varphi\} \\ = \alpha^a \rho^a g_k + \Theta_k^a + v_k^i \Psi^a. \end{aligned} \quad (40)$$

Herein α^s is the solid surface area per volume in the porous medium.

The energy balance for the solid phase is

$$\partial_t \{\alpha^s \rho^s u^s\} + \nabla \cdot \{\alpha^s \mathbf{q}^s\} = \Phi^s, \quad (41)$$

where u^s is the internal energy of the solid phase, \mathbf{q}^s is the heat flux and Φ^s accounts for heat transfer from the fluid phases. For the gas and adsorbed phases, the total energy is $e^j = u^j + v^j \cdot v^j/2$. For the solid, $e^s = u^s$. The total density of all the phases is $\rho = \sum_j \alpha^j \rho^j$. Correspondingly, the total internal energy is $\rho u = \sum_j \alpha^j \rho^j u^j$ and $\rho e = \sum_j \alpha^j \rho^j e^j$.

The balance equation for the total energy of all phases is

$$\begin{aligned} \partial_t \{\rho e\} + \nabla \cdot \sum_{j \in \{g,a\}} \{\alpha^j \rho^j e^j \mathbf{v}^j + \alpha^j \rho^j \mathbf{v}^j\} + \nabla \cdot \{\alpha^s \rho^s \mathbf{v}^s\} + \nabla \cdot \sum_j \{\alpha^j \mathbf{q}^j\} \\ = \alpha^g \rho^g \mathbf{g} \cdot \mathbf{v}^g + \alpha^a \rho^a \mathbf{g} \cdot \mathbf{v}^a, \end{aligned} \quad (42)$$

where \mathbf{q}^j is the heat flux through phase j . The heat flux through the gas phase is [48]

$$\mathbf{q}^g = \tilde{\mathbf{q}}^g + \sum_{i=1}^M h_i^g \tilde{\mathbf{j}}_i^g, \quad (43)$$

and, for the adsorbed and solid phases, it is

$$q^j = \tilde{q}^j, \quad (44)$$

where \tilde{q}^j is the measurable heat flux and h_i^s is the partial specific enthalpy.

Combining the mass and momentum balances, one may obtain a balance equation for the kinetic energy of the gas and the adsorbed phases. We now make the choice $v_k^i = \{v_k^a + v_k^s\} / 2$, on the grounds that this does not dissipate total kinetic energy, and subtract the kinetic energy balances from the total energy balance and get the balance equation for the internal energy

$$\begin{aligned} \partial_t \{\rho u\} + \partial_k \sum_{j \in \{g,a\}} \left\{ \alpha^j \rho^j v^j v_k^j \right\} + \partial_k \sum_j \left\{ \alpha^j q_k^j \right\} \\ = - \sum_{j \in \{g,a\}} \left\{ p \partial_k \left\{ \alpha^j v_k^j \right\} + v_k^j \Theta_k^j \right\} - \varphi \partial_k \left\{ \alpha^s v_k^s \right\}. \end{aligned} \quad (45)$$

The terms on the right hand side are due to mechanical volume work, viscous dissipation and interfacial work, respectively. The internal energy equation may be rewritten in terms of an equation for the enthalpy $\rho h = \sum_j \alpha^j \rho^j h^j$,

$$\begin{aligned} \partial_t \{\rho h\} + \partial_k \sum_{j \in \{g,a\}} \left\{ \alpha^j \rho^j h^j v_k^j \right\} + \partial_k \sum_j \left\{ \alpha^j q_k^j \right\} \\ = \partial_t \{p\} + \sum_{j \in \{g,a\}} \left\{ \alpha^j v_k^j \partial_k \{p\} - v_k^j \Theta_k^j \right\} + a^s \partial_t \{\varphi\} + \alpha^s v_k^a \partial_k \{\varphi\}. \end{aligned} \quad (46)$$

3.1. The entropy balance

To evaluate the consistency of the governing equations for transport through the porous medium, we will next derive the local entropy production. The second law of thermodynamics requires that this quantity is always non-negative.

We assume that the following thermodynamic Gibbs relations hold, which means local equilibrium for each phase.

$$du^a = T ds^a + \frac{p}{\{\rho^a\}^2} d\rho^a + \frac{\varphi}{\Gamma^2} d\Gamma, \quad (47)$$

$$du^s = T ds^s + \frac{p}{\{\rho^s\}^2} d\rho^s + \sum_{i=1}^M \mu_i d w_i^s, \quad (48)$$

$$du^s = T ds^s. \quad (49)$$

Inserting the Gibbs relations and the definition of the partial specific enthalpy,

$$h_i^j = T s_i^j - \mu_i, \quad (50)$$

into the balance equation for internal energy (45), we obtain a balance equation for the entropy,

$$\partial_t \{\rho s\} + \nabla \cdot \mathbf{j}_s = \sigma. \quad (51)$$

Herein, $\rho s = \sum_j \alpha^j \rho^j s^j$, the entropy flux is

$$\mathbf{j}_s = \sum_{j \in \{g,a\}} \left\{ \alpha^j \rho^j s^j \mathbf{v}^j + \frac{\alpha^j \tilde{q}^j}{T} \right\} + \alpha^s \sum_{i=1}^M s_i^s \tilde{\mathbf{j}}_i^s + \frac{\alpha^s \tilde{q}^s}{T}, \quad (52)$$

and, using Eqs. (43), (44) and (50), we can formulate the entropy production as

$$\sigma = \nabla \cdot \left\{ \frac{1}{T} \right\} \cdot \tilde{\mathbf{q}} + \sum_{i=1}^M \left(\frac{-\nabla_T \mu_i}{T} \right) \cdot \tilde{\mathbf{j}}_i - \sum_{j \in \{g,a\}} \frac{v_k^j \Theta_k^j}{T}. \quad (53)$$

The symbol ∇_T means that variations in temperature are omitted when evaluating the gradient. Also, $\tilde{\mathbf{j}}_i = \alpha^s \tilde{\mathbf{j}}_i^s$ is the total diffusive mass flux of component i and $\tilde{\mathbf{q}} = \sum_j \alpha^j \tilde{q}^j$ is the total measurable heat flux. The three terms on the right-hand side of Eq. (53) can thus be attributed

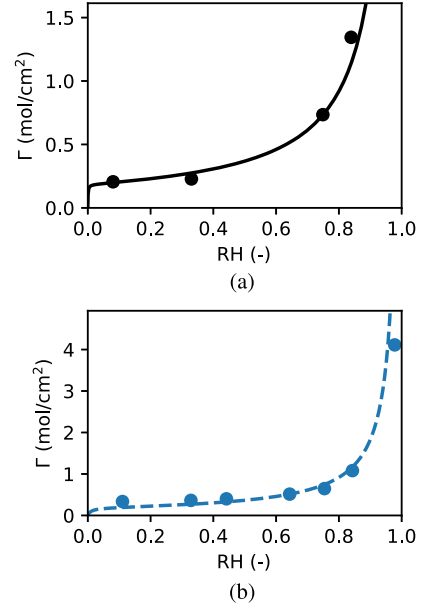


Fig. 1. Fitted (temperature-independent) BET models for (a) the L2 data set from [55] and (b) the CNR data set from [56].

to, respectively, measurable heat flux, diffusive mass flux and viscous dissipation.

4. Case studies: transport of moisture in porous insulation materials

In this section, we will present the example cases discussed in Sec. 5. As a simple yet timely example [55], we consider moisture transport in porous insulation materials that includes adsorption of water onto and into the porous matrix.

In all simulated cases, the adsorption is described by a temperature-independent BET model fitted to the L2 data set from [55], obtained from measurements with glass wool (see Fig. 1a). We have also fitted the BET model to the CNR data set from [56], obtained from a mineral wool with hydrophobic admixture (see Fig. 1b), to have an additional example when discussing the thermodynamic properties of the adsorbed phase. For both data sets, the parameters $a = 0.18 \text{ mol cm}^{-2}$ and $c = 0.999$ were used, and ξ was fitted to 1388 and 106 for the L2 and CNR isotherms, respectively. When discussing adsorption of water, it is common practice to use relative humidity RH in place of the dimensionless partial pressure \hat{p}_1 and we will therefore use RH in the following. An area per adsorbed molecule of $(0.3 \text{ nm})^2$ has been assumed, so that the adsorption area per volume of insulation is $a^s = 6.39 \times 10^5 \text{ m}^2 \text{ m}^{-3}$.

We use the following correlation for the saturation pressure of water:

$$p^{\text{sat}}(T) = 1 \text{ Pa} \times \exp \left(77.345 + 0.0057 \text{ K}^{-1} T - \frac{7235 \text{ K}}{T} \right) \times \left\{ \frac{1 \text{ K}}{T} \right\}^{8.2} \quad (54)$$

The thermodynamic models describing the gas, solid and bulk liquid properties are listed in the SI. Both the liquid and solid phases are approximated as incompressible and the air is treated as an ideal two-component mixture of water and a single pseudo-component representing dry air.

4.1. Equilibrium case

In this section, we describe a case where a piece of highly porous, humid insulation material is heated at constant pressure. The heating is assumed to occur reversibly, such that the system is in equilibrium with the environment at all times, and there are no internal driving forces in the system. This case will therefore be referred to as *the equilibrium case*.

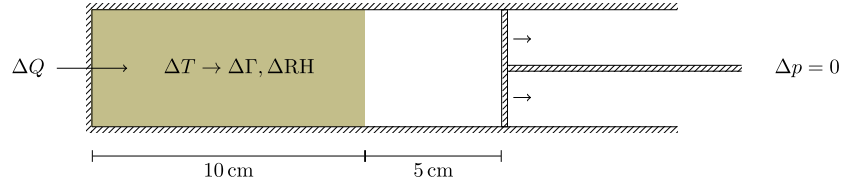


Fig. 2. Schematic illustration of the equilibrium case. A piece of porous insulation (beige) is heated by adding an amount of heat ΔQ . During the process, the gas is allowed to expand so that $\Delta p = 0$. The addition of heat leads to an increase in temperature ΔT and resulting changes in adsorption $\Delta \Gamma$ and relative humidity ΔRH .

The case and the numerical results will be used to discuss the effect of incorporating a consistent thermodynamic description of the adsorbed phase on the temperature evolution during a constant-pressure adsorption/desorption process.

We consider a closed container with a piece of porous material occupying a part of its volume, as illustrated in Fig. 2. The porous material contains a solid phase and an adsorbed phase, in addition to a gas phase. The container has a cross section of $10 \text{ cm} \times 10 \text{ cm}$ and an initial total length of 15 cm . The porous material occupies 10 cm of its length and the additional 5 cm consists of a gas-filled head space that can change its volume to keep the pressure constant at 10^5 Pa . Initially, the relative humidity is 0.6 and the temperature is 300 K .

The container is then heated by adding the amount of heat ΔQ . The container remains closed, but the head space is allowed to expand in volume so that the pressure remains constant, i.e. $\Delta p = 0$. We assume chemical equilibrium at all times, i.e. $\mu_{\text{H}_2\text{O}}^g = \mu^a$. The amount of porous material in the container is fixed, so the adsorption area remains unchanged $\Delta A = 0$ and, since the container is closed, any desorbing water enters the gas phase, i.e. $\Delta N^a = -\Delta N_{\text{H}_2\text{O}}^g$ and the amount of air in the gas phase does not change, $\Delta N_{\text{air}}^g = 0$.

To assess the influence of a temperature-dependence of the adsorption, we use a linearization of the temperature dependence of the L2 adsorption, as described by Eq. (33), and perform calculations from different values of the parameter β .

4.2. Non-equilibrium case

To study non-isothermal transport in the porous insulation material, we will consider a one-dimensional, horizontal case and therefore set the gravitational acceleration to zero. The adsorbed phase is furthermore assumed not to flow, so that $j_{\text{H}_2\text{O}}^a = \mathbf{0}$. Mass transport of water will then only occur through the gas phase. Heat can flow through all three phases.

We assume gas flow at low Reynolds numbers and therefore choose to model the viscous friction force to be proportional to the gas flow velocity v_k^g and the gas viscosity η^g ,

$$\sigma_k^g = -\alpha^g \eta^g v_k^g / \kappa. \quad (55)$$

This choice of model defines the permeability κ of the insulation. We assume instant relaxation to steady-state flow and neglect the contribution from $v_k^i \Psi^g$ in the gas momentum equation (39). Furthermore, the low Reynolds number assumption means that the inertial term can also be omitted. Equation (39) then reduces to Darcy's law.

The diffusive transport of mass is modeled using Fick's law,

$$\tilde{j}_{\text{H}_2\text{O}}^g = -\rho^g D \nabla w_{\text{H}_2\text{O}}^g. \quad (56)$$

Herein, the diffusion coefficient is modeled by

$$D(T) = 1.97 \times 10^{-5} \text{ m}^2 \text{ s}^{-1} \times \left\{ \frac{T}{256 \text{ K}} \right\}^{1.685}. \quad (57)$$

The total measurable heat flux, through all phases, is modeled by Fourier's law,

$$\tilde{q} = -\lambda \nabla T, \quad (58)$$

Table 1

Transport properties of the porous insulation used in the non-equilibrium cases.

Quantity	Symbol	Value	Unit
Permeability	κ	3×10^{-10}	m^2
Thermal conductivity	λ	5.4×10^{-2}	$\text{W m}^{-1} \text{ K}^{-1}$
Gas viscosity	η^g	1.8×10^{-5}	Pa s

where λ is the bulk thermal conductivity of the insulation material. We choose to model the total heat flux because the thermal conductivity of insulation materials is most often measured as a bulk property and not as contributions from the individual phases. The values of the transport properties used in the non-equilibrium case are provided in Table 1 and the numerical solution procedure used is outlined in Appendix A.

We shall here consider a non-equilibrium warm-up case where the domain is heated from one side and heat and mass transport is driven mainly by a sensible heat flux over one boundary. The main purpose of this case is to show that a consistent thermodynamic description of the adsorbed phase is required to arrive at a model for transport that satisfies the second law of thermodynamics. In the SI, we also consider a diffusion case where heat and mass transfer is driven by a concentration difference.

A schematic illustration of the warm-up case is shown in Fig. 3. We consider a one-dimensional domain that is 10 cm in length. Initially, there is a temperature of 300 K , a pressure of 10^5 Pa and a relative humidity of 0.3 . The domain is open on the eastern side where the initial values are applied as boundary conditions. On the western side, there is a wall boundary (with no mass flow across it) and a constant temperature of 310 K that causes the domain to warm up. Simulations were run from $t = 0 \text{ s}$ to $t = 240 \text{ s}$.

5. Results and discussion

5.1. The thermodynamic properties of water adsorbed in insulation materials

We will first discuss the thermodynamic properties of the adsorbed phase, calculated using the temperature-independent BET model fitted to the L2 data set from [55] (see Fig. 1a) and the CNR data set from [56] (see Fig. 1b) as adsorption models.

The resulting chemical potential difference between the adsorbed phase and a bulk liquid phase is plotted against the relative humidity in Fig. 4. As is evident from Eq. (23), this curve is the same for all choices of adsorption model. The difference between the adsorbed-phase and bulk-phase chemical potential is zero at saturation ($RH = 1$). At relative humidities below 1, the chemical potential of the adsorbed phase is lower than that of a bulk liquid phase at saturation, and equilibrium co-existence of an adsorbed phase with a gas phase is therefore possible.

The difference in enthalpy and entropy between the adsorbed phase and the bulk liquid phase are shown in Fig. 5. At relative humidities below 1, both the L2 and CNR temperature-independent isotherms give enthalpies and entropies that are higher than that of the bulk liquid phase. At saturation, the differences between the adsorbed phases and the bulk liquid phase disappear, as expected. It is, however, not evident how a change in the enthalpy of the adsorbed phase affects the

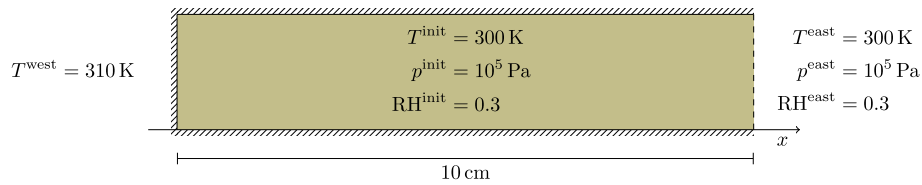


Fig. 3. Schematic illustrations of boundary and initial conditions in the warm-up case.

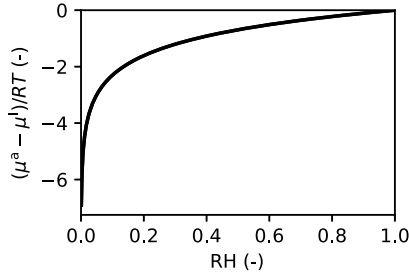


Fig. 4. Difference between the chemical potential of the adsorbed phase and liquid phase.

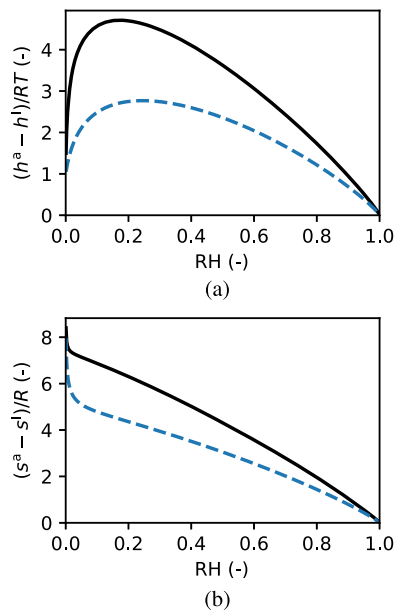


Fig. 5. Differences in (a) enthalpy and (b) entropy between the adsorbed phase and the bulk liquid phase for the L2 isotherm (solid black) and the CNR isotherm (dashed blue). (For interpretation of the colors in the figure(s), the reader is referred to the web version of this article.)

temperature evolution during adsorption. The reason for this is that the spreading pressure also enters into the thermodynamic description. This will be discussed in greater detail in Sec. 5.2.

5.2. Equilibrium case: the thermal effects of adsorption/desorption at constant pressure

In this section, we will discuss the equilibrium case described in Sec. 4.1. The purpose is to clarify how the adsorption thermodynamics influences the temperature in the porous medium.

Unless the adsorption model has an explicit temperature dependence, there is no difference in the temperature evolution during adsorption/desorption between the bulk model and the consistent thermodynamic description of the adsorbed phase. In the SI, we make this argument by analytical means. Here we illustrate the same point by numerically evaluating the connection between the heat ΔQ added and

the resulting temperature change ΔT . As it turns out, there is a one-to-one mapping between the heat ΔQ added to the system and the resulting temperature change ΔT . In the SI, we show this analytically for small perturbations. For the present case this holds also for larger changes, as can be seen in Fig. 6a, where ΔQ is plotted against ΔT . Furthermore, for all values of β , the temperature increases when heat is added and decreases if heat is removed.

To isolate the effect of the temperature dependence of the adsorption on the temperature response in the porous medium, we consider ΔQ with the bulk-phase enthalpy changes subtracted. This is plotted in Fig. 6b. It is clear that when the adsorption has no explicit temperature dependence ($\beta = 0$), the temperature response is given by the bulk-phase enthalpy, since the line with $\beta = 0$ is constant and equal to zero. This means that there will be no difference in the temperature change predicted if the bulk phase model was used in place of the consistent thermodynamic framework. This is in-line with the analytical arguments in the SI. When $\beta \neq 0$, on the other hand, then, depending on the sign of β , the heat required to produce a given temperature increase can be both larger and smaller than that predicted using the bulk-phase description of the adsorbed phase. Negative values of β mean that more heat is needed and positive values means that less heat is needed. Correspondingly, more heat must be removed the system to reduce the temperature when β is negative and less must be removed when it is positive.

The change in adsorption $\Delta \Gamma$ is plotted in Fig. 6c and the change in relative humidity ΔRH is shown in Fig. 6d. For this case, there is a similar response in adsorption to temperature change for the different values of β . The change in relative humidity, on the other hand, is qualitatively different for different values of β and the relative humidity may increase or decrease in response to a temperature increase, depending on the β value.

In summary, the equilibrium case highlights the importance of characterizing the temperature dependence of the adsorption by use of experiments or molecular simulations for accurate non-isothermal modeling of porous media.

5.3. Non-equilibrium case: the second law of thermodynamics

The non-equilibrium warm-up case was described in Sec. 4.2. We have simulated this case numerically, as explained in Appendix A, using both the consistent thermodynamic framework and the bulk liquid model for the adsorbed phase. The resulting temperature, relative humidity, pressure, volume fraction of adsorbed water and mass fraction of water in the gas phase after 0 s, 120 s and 240 s, using the consistent thermodynamic description of the adsorbed phase, are shown in Fig. 7. Initially, there is a uniform state in the insulation material and a higher temperature on the western boundary. As the simulation progresses, the western end of the domain is warmed up by the wall (see Fig. 7a) and, as a result of this temperature increase, the relative humidity drops near the western wall (see Fig. 7b). This drop in relative humidity causes desorption near the wall (see Fig. 7c) and release of adsorbed water into the gas phase. The combined effect of desorption and temperature increase, causes a small increase in pressure near the heated wall. The pressure gradient and the gradient in water mass fraction (see Fig. 7d) both cause transport of water away from the heated wall and further into the domain. When the transported water eventually reaches a colder region, the relative humidity increases, leading to

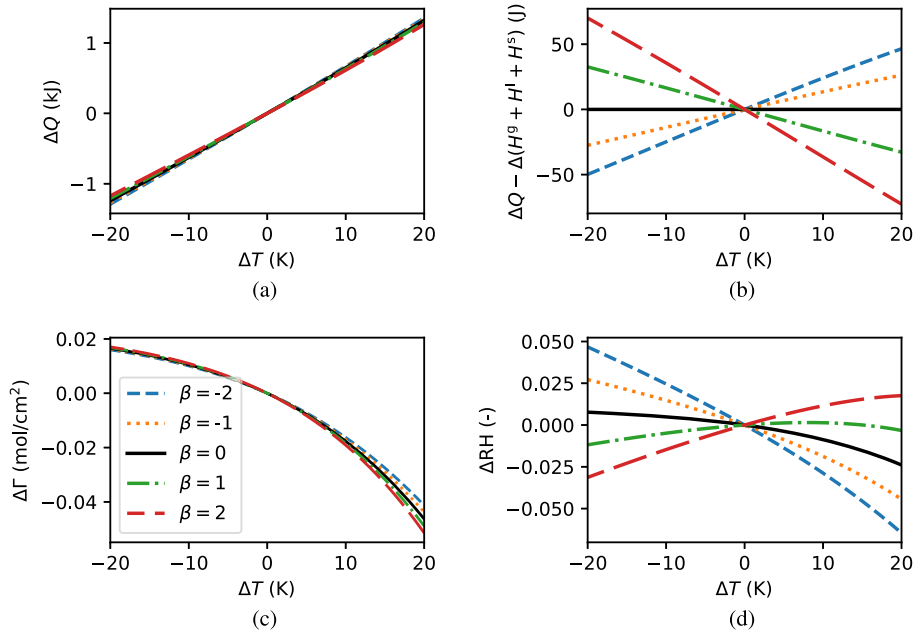


Fig. 6. Numerical results from the equilibrium case for different values of the parameter β , describing the explicit temperature dependence of the adsorption model. The temperature-independent adsorption model corresponds to $\beta = 0$. (a) Heat ΔQ needed to produce temperature change ΔT . (b) Difference between heat ΔQ and the change in bulk enthalpy. (c) Change in adsorption $\Delta\Gamma$ in response to temperature change. (d) Change in relative humidity ΔRH in response to a temperature change.

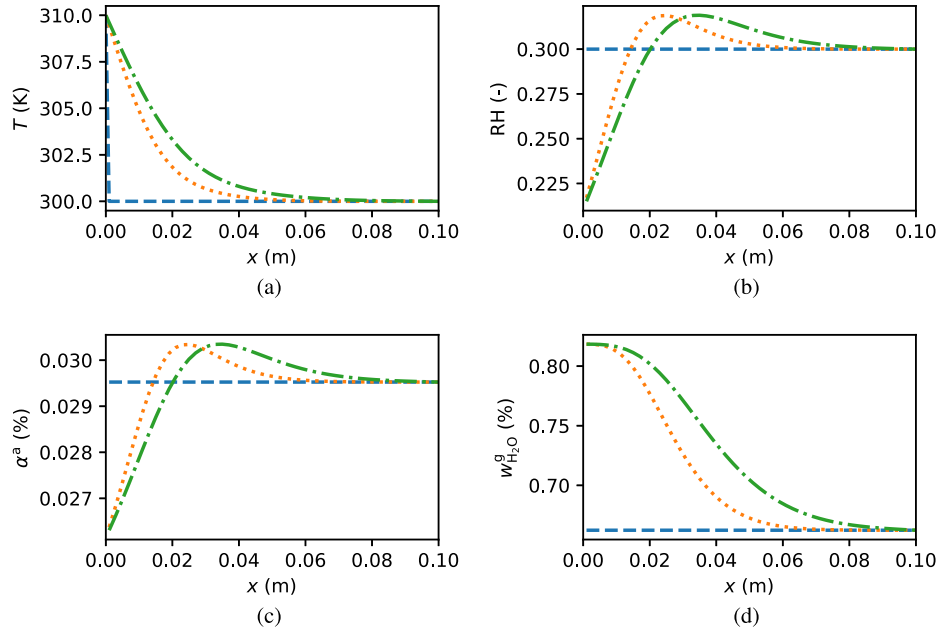


Fig. 7. Results from the warm-up case at $t = 0$ s (dashed blue), $t = 120$ s (dotted orange) and $t = 240$ s (dash-dotted green).

relative humidity values and amounts of adsorbed water in excess of the initial level (see Fig. 7b and Fig. 7c). This is as expected for the temperature-independent adsorption model used.

When the balance equations are solved with the bulk liquid model in place of the consistent model for the adsorbed phase, there is no discernible difference in the profiles in Fig. 7. This is as expected for the temperature-independent adsorption model used.

The contributions to the entropy production at $t = 240$ s from the three terms in Eq. (53), viscous friction, sensible heat flux and mass flux, are illustrated in Fig. 8. The dominant contribution in this case is from the sensible heat flux, while there is a smaller contribution from the mass flux. The contribution from viscous dissipation is negligible.

Fig. 9 shows the local entropy production σ from Eq. (53) at $t = 240$ s. This corresponds to the right-hand side of the entropy balance in equation, Eq. (51). Also shown is the left-hand side of Eq. (51). If the description of the porous medium is consistent with the second law of thermodynamics, the left- and right-hand sides of the entropy balance equation must be equal and non-negative. Fig. 9a shows that, when using the consistent thermodynamic description for the adsorbed phase, the entropy balance equation is satisfied and the entropy production is non-negative everywhere. For the bulk liquid model, on the other hand, we see from Fig. 9b that the entropy balance equation is not satisfied. Furthermore, the left-hand side is negative in some parts of the domain and the model thus violates the second law of thermodynamics.

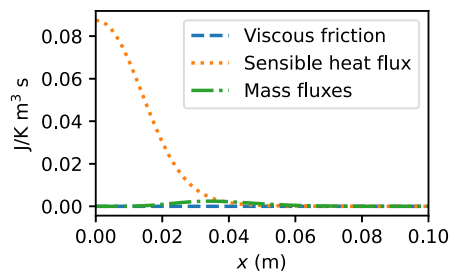


Fig. 8. Contributions to entropy production at $t = 240$ s for the warm-up case.

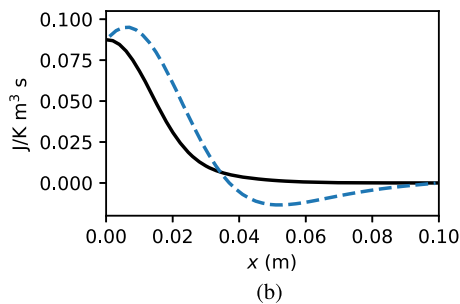
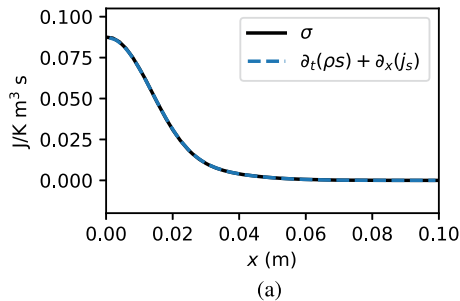


Fig. 9. Entropy balance at $t = 240$ s in the warm-up case using (a) the thermodynamically consistent framework and (b) the bulk liquid model for the adsorbed phase.

The reason for the thermodynamic inconsistency is evident by comparing the chemical potential of water in the adsorbed phase and the gas phase. In Fig. 10, these are plotted at $t = 240$ s. For the thermodynamically consistent framework, the chemical potential of water is the same in the gas and the adsorbed phase, consistent with the assumption of chemical equilibrium. For the bulk-liquid model, however, the chemical potential of the adsorbed phase does not match that of water in the gas phase. The discrepancy between the right- and left-hand sides of the entropy balance equation Fig. 9b can be attributed to this mismatch of chemical potentials.

In the SI, we consider an additional non-equilibrium case where the mass fluxes rather than the sensible heat flux are the main contribution to the entropy production. Also in this case, the second law of thermodynamics is violated if the bulk liquid model is used in place of the consistent thermodynamic description of the adsorbed phase.

6. Conclusion

Sorption in porous media and the resulting thermal effects are of key relevance to a wide range of examples such as capture of CO_2 and storage of hydrogen with zeolites or metal organic frameworks, drying of soil in agriculture, and drying of pharmaceutical materials, food, paint and coal. Due to lack of experimental data and reliable models, a common assumption is that the thermodynamic properties of the adsorbed phase are the same as those of the bulk fluid. In this work, we have used non-isothermal, gaseous transport of moist air through a porous insulation material as an example to show that this assumption leads to

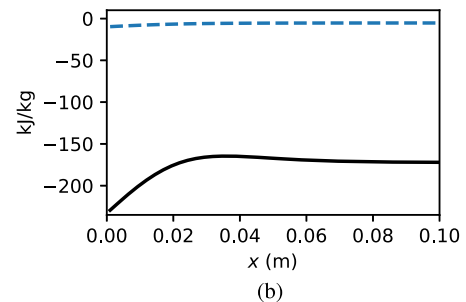
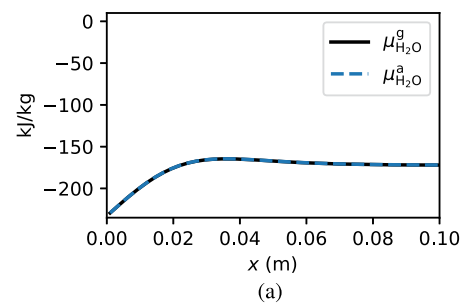


Fig. 10. Chemical potentials at $t = 240$ s in the warm-up case using (a) the thermodynamically consistent framework and (b) the bulk liquid model for the adsorbed phase.

violation of the second law of thermodynamics and a negative entropy production.

To remedy this, we have derived a consistent thermodynamic framework for single-component adsorbed phases in contact with ideal gases, which is based on a work by T. Hill from 1949 [38]. The advantage of the derived framework is that it is self-consistent with the model or data used to describe the sorption isotherm(s) and the thermodynamic properties of the bulk fluids. From the framework, we obtain thermodynamic properties such as the chemical potential, enthalpy and entropy. Motivated by the present lack of predictive models, we argue that the resulting chemical potential can be used as a starting point in consistent and accurate models for adsorption kinetics based on non-equilibrium thermodynamics.

By combining the consistent thermodynamic framework for the adsorbed phase with the balance equations for energy, entropy and momentum through the porous medium, we show that the entropy balance is fulfilled and that the entropy production is positive, in agreement with the second law of thermodynamics. A key finding is that the temperature evolution in the porous medium from the consistent description differs from the standard formulation only if the adsorption depends explicitly on temperature. This highlights the importance of characterizing the temperature dependence of the adsorption by use of experiments or molecular simulations for accurate non-isothermal modeling of porous media.

CRediT authorship contribution statement

Magnus Aa. Gjennestad: Writing – review & editing, Writing – original draft, Visualization, Validation, Software, Methodology, Investigation, Formal analysis. **Øivind Wilhelmsen:** Writing – review & editing, Writing – original draft, Supervision, Software, Methodology, Investigation, Formal analysis, Conceptualization.

Declaration of competing interest

The authors declare that they have no known competing financial interests or personal relationships that could have appeared to influence the work reported in this paper.

Data availability

Data will be made available on request.

Acknowledgements

The authors would like to thank Ole Meyer and Åsmund Ervik for fruitful discussions. This work was supported by the PredictCUI project coordinated by SINTEF Energy Research, and the authors acknowledge the contributions of Equinor, Gassco, Shell and the PETROMAKS 2 programme of the Research Council of Norway (308770). Furthermore, Øivind Wilhelmsen acknowledges support by the Research Council of Norway through its Centres of Excellence funding scheme (262644).

Appendix A. Numerical solution of the non-equilibrium case

With the assumptions made in Sec. 4.2, the transport equations to be solved reduced to two partial differential equations (PDEs) for mass, one for water and one for air, and one PDE for enthalpy. These were spatially discretized with the finite volume method (FVM) [57] on a one-dimensional grid with 50 uniform cells, producing a system of coupled ordinary differential equations (ODEs). Evaluation of the right-hand-side of the ODEs required computation of temperature, pressure, amount of adsorbed water etc. in each grid cell from the total component masses and total enthalpy in each cell, assuming local equilibrium and that the amount for adsorbed water was given by the BET model. This involved solving two non-linear equations for each grid cell using Newton's method [58]. The ODEs were integrated in time using the backward Euler method [58] and a time step of 1 s. Each time step was solved as a system of non-linear equations using the Scalable Nonlinear Equations Solvers (SNES) component the PETSc library [59,60], with `fsolve` from the `optimize` module of SciPy [61] as a fallback.

Appendix B. Supplementary material

Supplementary material related to this article can be found online at <https://doi.org/10.1016/j.ijheatmasstransfer.2024.125462>.

References

- [1] M. Bidner, P. Porcelli, Influence of capillary pressure, adsorption and dispersion on chemical flood transport phenomena, *Transp. Porous Media* 24 (1996) 275–296, <https://doi.org/10.1007/BF00154094>.
- [2] Z. Lv, P. Liu, Y. Zhao, Experimental study on the effect of gas adsorption on the effective stress of coal under triaxial stress, *Transp. Porous Media* 137 (2021) 365–379, <https://doi.org/10.1007/s11242-021-01564-8>.
- [3] H. Seomoon, M. Lee, W. Sung, Analysis of sorption-induced permeability reduction considering gas diffusion phenomenon in coal seam reservoir, *Transp. Porous Media* 108 (2015) 713–729, <https://doi.org/10.1007/s11242-015-0498-5>.
- [4] K.M. Thomas, Hydrogen adsorption and storage on porous materials, *Catal. Today* 120 (3–4) (2007) 389–398, <https://doi.org/10.1016/j.cattod.2006.09.015>.
- [5] R. Paggiaro, P. Bénard, W. Polifke, Cryo-adsorptive hydrogen storage on activated carbon. I: Thermodynamic analysis of adsorption vessels and comparison with liquid and compressed gas hydrogen storage, *Int. J. Hydrog. Energy* 35 (2) (2010) 638–647, <https://doi.org/10.1016/j.ijhydene.2009.10.108>, <https://www.sciencedirect.com/science/article/pii/S0360319909017376>.
- [6] Z. Chen, K.O. Kirlikovali, K.B. Idrees, M.C. Wasson, O.K. Farha, Porous materials for hydrogen storage, *Chem* 8 (3) (2022) 693–716, <https://doi.org/10.1016/j.chempr.2022.01.012>, <https://www.sciencedirect.com/science/article/pii/S2451929422000420>.
- [7] S. Kumar, R. Srivastava, J. Koh, Utilization of zeolites as CO₂ capturing agents: advances and future perspectives, *J. CO₂ Utilization* 41 (2020) 101251, <https://doi.org/10.1016/j.jcou.2020.101251>, <https://www.sciencedirect.com/science/article/pii/S2212982020303863>.
- [8] B. Wei, X. Zhang, J. Liu, X. Xu, W. Pu, M. Bai, Adsorptive behaviors of supercritical CO₂ in tight porous media and triggered chemical reactions with rock minerals during CO₂-EOR and -sequestration, *Chem. Eng. J.* 381 (2020) 122577, <https://doi.org/10.1016/j.cej.2019.122577>.
- [9] J.H. Choe, H. Kim, C.S. Hong, MOF-74 type variants for CO₂ capture, *Mater. Chem. Front.* 5 (14) (2021) 5172–5185, <https://doi.org/10.1039/D1QM00205H>, <https://pubs.rsc.org/en/content/articlelanding/2021/qm/d1qm00205h>.
- [10] S. Deutz, A. Bardow, Life-cycle assessment of an industrial direct air capture process based on temperature-vacuum swing adsorption, *Nat. Energy* 6 (2) (2021) 203–213, <https://doi.org/10.1038/s41560-020-00771-9>.
- [11] L. Riboldi, O. Bolland, Overview on pressure swing adsorption (PSA) as CO₂ capture technology: state-of-the-art, limits and potentials, *Energy Proc.* 114 (2017) 2390–2400, <https://doi.org/10.1016/j.egypro.2017.03.1385>, <https://www.sciencedirect.com/science/article/pii/S1876610217315709>.
- [12] S.E. Zanco, M. Mazzotti, M. Gazzani, M.C. Romano, I. Martínez, Modeling of circulating fluidized beds systems for post-combustion CO₂ capture via temperature swing adsorption, *AIChE J.* 64 (5) (2018) 1744–1759, <https://doi.org/10.1002/aic.16029>.
- [13] L. Chen, S. Deng, R. Zhao, Y. Zhu, L. Zhao, S. Li, Temperature swing adsorption for CO₂ capture: thermal design and management on adsorption bed with single-tube/three-tube internal heat exchanger, *Appl. Therm. Eng.* 199 (2021) 117538, <https://doi.org/10.1016/j.applthermaleng.2021.117538>.
- [14] C.J. Simonson, M. Salonvaara, T. Ojanen, The effect of structures on indoor humidity – possibility to improve comfort and perceived air quality, *Indoor Air* 12 (4) (2002) 243–251, <https://doi.org/10.1034/j.1600-0668.2002.01128.x>.
- [15] O. Kolditz, J. De Jonge, Non-isothermal two-phase flow in low-permeable porous media, *Comput. Mech.* 33 (5) (2004) 345–364, <https://doi.org/10.1007/s00466-003-0537-x>.
- [16] Z. Pavlík, J. Žumár, I. Medved, R. Černý, Water vapor adsorption in porous building materials: experimental measurement and theoretical analysis, *Transp. Porous Media* 91 (2012) 939–954, <https://doi.org/10.1007/s11242-011-9884-9>.
- [17] X. Liu, Y. Chen, H. Ge, P. Fazio, G. Chen, X. Guo, Determination of optimum insulation thickness for building walls with moisture transfer in hot summer and cold winter zone of China, *Energy Build.* 109 (2015) 361–368, <https://doi.org/10.1016/j.enbuild.2015.10.021>.
- [18] Y.-K. Yeo, K.-S. Hwang, S.C. Yi, H. Kang, Modeling of the drying process in paper plants, *Korean J. Chem. Eng.* 21 (4) (2004) 761–766, <https://doi.org/10.1007/BF02705517>.
- [19] A. Etemoglu, M. Can, A. Avci, E. Pulat, Theoretical study of combined heat and mass transfer process during paper drying, *Heat Mass Transf.* 41 (2005) 419–427, <https://doi.org/10.1007/s00231-004-0538-0>.
- [20] W. Wu, B. Wang, W. Shi, X. Li, Absorption heating technologies: a review and perspective, *Appl. Energy* 130 (2014) 51–71, <https://doi.org/10.1016/j.apenergy.2014.05.027>.
- [21] J. Heitman, R. Horton, T. Sauer, T. Ren, X. Xiao, Latent heat in soil heat flux measurements, *Agric. For. Meteorol.* 150 (7–8) (2010) 1147–1153, <https://doi.org/10.1016/j.agrformet.2010.04.017>.
- [22] Z. Li, J. Vanderborght, K.M. Smits, Evaluation of model concepts to describe water transport in shallow subsurface soil and across the soil-air interface, *Transp. Porous Media* 128 (2019) 945–976, <https://doi.org/10.1007/s11242-018-1144-9>.
- [23] Z. Erbay, F. Icier, A review of thin layer drying of foods: theory, modeling, and experimental results, *Crit. Rev. Food Sci. Nutr.* 50 (5) (2010) 441–464, <https://doi.org/10.1080/10408390802437063>.
- [24] M.M. Rahman, M.U. Joardder, M.I.H. Khan, N.D. Pham, M. Karim, Multi-scale model of food drying: current status and challenges, *Crit. Rev. Food Sci. Nutr.* 58 (5) (2018) 858–876, <https://doi.org/10.1080/10408398.2016.1227299>.
- [25] R.H. Walters, B. Bhatnagar, S. Tchessalov, K.-I. Izutsu, K. Tsumoto, S. Ohtake, Next generation drying technologies for pharmaceutical applications, *J. Pharm. Sci.* 103 (9) (2014) 2673–2695, <https://doi.org/10.1002/jps.23998>.
- [26] L. Xu, S. Davies, A.B. Schofield, D.A. Weitz, Dynamics of drying in 3D porous media, *Phys. Rev. Lett.* 101 (9) (2008) 094502, <https://doi.org/10.1103/PhysRevLett.101.094502>.
- [27] S. Howison, J. Moriarty, J. Ockendon, E. Terrill, S. Wilson, A mathematical model for drying paint layers, *J. Eng. Math.* 32 (1997) 377–394, <https://doi.org/10.1023/A:1004224014291>.
- [28] Z. Chen, W. Wu, P. Agarwal, Steam-drying of coal. Part 1. Modeling the behavior of a single particle, *Fuel* 79 (8) (2000) 961–974, [https://doi.org/10.1016/S0016-2361\(99\)00217-3](https://doi.org/10.1016/S0016-2361(99)00217-3).
- [29] M.Aa. Gjennestad, Ø. Wilhelmsen, Thermodynamic stability of droplets, bubbles and thick films in open and closed pores, *Fluid Phase Equilib.* 505 (2020) 112351, <https://doi.org/10.1016/j.fluid.2019.112351>.
- [30] M. Steeman, A. Janssens, H.-J. Steeman, M. Van Belleghem, M. De Paepe, On coupling 1D non-isothermal heat and mass transfer in porous materials with a multizone building energy simulation model, *Build. Environ.* 45 (4) (2010) 865–877, <https://doi.org/10.1016/j.buildenv.2009.09.006>.
- [31] M. Van Belleghem, H.-J. Steeman, M. Steeman, A. Janssens, M. De Paepe, Sensitivity analysis of CFD coupled non-isothermal heat and moisture modelling, *Build. Environ.* 45 (11) (2010) 2485–2496, <https://doi.org/10.1016/j.buildenv.2010.05.011>.
- [32] W.G. Gray, C.T. Miller, Thermodynamically constrained averaging theory approach for modeling flow and transport phenomena in porous medium systems: 1. Motivation and overview, *Adv. Water Resour.* 28 (2) (2005) 161–180, <https://doi.org/10.1016/j.advwatres.2004.09.005>.
- [33] C.T. Miller, W.G. Gray, Thermodynamically constrained averaging theory approach for modeling flow and transport phenomena in porous medium systems: 2. Foundation, *Adv. Water Resour.* 28 (2) (2005) 181–202, <https://doi.org/10.1016/j.advwatres.2004.09.006>.

- [34] M. Torabi, N. Karimi, G. Peterson, S. Yee, Challenges and progress on the modelling of entropy generation in porous media: a review, *Int. J. Heat Mass Transf.* 114 (2017) 31–46, <https://doi.org/10.1016/j.ijheatmasstransfer.2017.06.021>.
- [35] W. Rose, Rate of entropy production questions associated with transport of coupled processes in and through the interstices of crack porous media systems, *Transp. Porous Media* 41 (1) (2000) 117–120, <https://doi.org/10.1023/A:1006681017735>.
- [36] F. Gay-Balmaz, V. Putkaradze, Variational geometric approach to the thermodynamics of porous media, *ZAMM - J. Appl. Math. Mech./Z. Angew. Math. Mech.* 102 (11) (2022), <https://doi.org/10.1002/zamm.202100198>.
- [37] F. Gay-Balmaz, V. Putkaradze, Thermodynamically consistent variational theory of porous media with a breaking component, *Contin. Mech. Thermodyn.* 36 (2023) 75–105, <https://doi.org/10.1007/s00161-023-01262-4>.
- [38] T.L. Hill, Statistical mechanics of adsorption. V. Thermodynamics and heat of adsorption, *J. Chem. Phys.* 17 (6) (1949) 520–535, <https://doi.org/10.1063/1.1747314>.
- [39] S. Kjelstrup, D. Bedeaux, E. Johannessen, J. Gross, *Non-equilibrium Thermodynamics for Engineers*, World Scientific, Singapore, 2017.
- [40] C. Clarkson, R. Bustin, J. Levy, Application of the mono/multilayer and adsorption potential theories to coal methane adsorption isotherms at elevated temperature and pressure, *Carbon* 35 (12) (1997) 1689–1705, [https://doi.org/10.1016/S0008-6223\(97\)00124-3](https://doi.org/10.1016/S0008-6223(97)00124-3).
- [41] P. Benard, R. Chahine, Determination of the adsorption isotherms of hydrogen on activated carbons above the critical temperature of the adsorbate over wide temperature and pressure ranges, *Langmuir* 17 (6) (2001) 1950–1955, <https://doi.org/10.1021/la001381x>.
- [42] K.S. Walton, A.R. Millward, D. Dubbeldam, H. Frost, J.J. Low, O.M. Yaghi, R.Q. Snurr, Understanding inflections and steps in carbon dioxide adsorption isotherms in metal-organic frameworks, *J. Am. Chem. Soc.* 130 (2) (2008) 406–407, <https://doi.org/10.1021/ja076595g>.
- [43] Y. Xie, C.A. Hill, Z. Jalaludin, S.F. Curling, R.D. Anandjiwala, A.J. Norton, G. Newman, The dynamic water vapour sorption behaviour of natural fibres and kinetic analysis using the parallel exponential kinetics model, *J. Mater. Sci.* 46 (2) (2011) 479–489, <https://doi.org/10.1007/s10853-010-4935-0>.
- [44] E.E. Thybring, C.R. Boardman, S.V. Glass, S.L. Zelinka, The parallel exponential kinetics model is unfit to characterize moisture sorption kinetics in cellulosic materials, *Cellulose* 26 (2) (2019) 723–735, <https://doi.org/10.1007/s10570-018-2134-3>.
- [45] R. Kohler, R. Dück, B. Ausperger, R. Alex, A numeric model for the kinetics of water vapor sorption on cellulosic reinforcement fibers, *Compos. Interfaces* 10 (2–3) (2003) 255–276, <https://doi.org/10.1163/156855403765826900>.
- [46] R. Kohler, R. Alex, R. Brielmann, B. Ausperger, A new kinetic model for water sorption isotherms of cellulosic materials, in: *Macromolecular Symposia*, vol. 244, 2006, pp. 89–96.
- [47] S. Tripathi, R.F. Tabor, Modeling two-rate adsorption kinetics: two-site, two-species, bilayer and rearrangement adsorption processes, *J. Colloid Interface Sci.* 476 (2016) 119–131, <https://doi.org/10.1016/j.jcis.2016.05.007>.
- [48] S. Kjelstrup, D. Bedeaux, *Non-equilibrium Thermodynamics of Heterogeneous Systems*, *Advances in Statistical Mechanics*, vol. 16, World Scientific, Singapore, 2010.
- [49] M.Aa. Gjennestad, Ø. Wilhelmsen, Thermodynamic stability of volatile droplets and thin films governed by disjoining pressure in open and closed containers, *Langmuir* 36 (27) (2020) 7879–7893, <https://doi.org/10.1021/acs.langmuir.0c00960>.
- [50] M.L. Michelsen, J.M. Mollerup, *Thermodynamic Models: Fundamentals and Computational Aspects*, 2nd edition, Tie-Line Publications, Holte, Denmark, 2007.
- [51] D.H. Bangham, The Gibbs adsorption equation and adsorption on solids, *Trans. Faraday Soc.* 33 (1937) 805–811, <https://doi.org/10.1039/tf9373300805>.
- [52] H.B. Callen, *Thermodynamics and an Introduction to Thermostatistics*, 2nd edition, John Wiley and Sons, New York, USA, 1985.
- [53] S. Brunauer, P.H. Emmett, E. Teller, Adsorption of gases in multimolecular layers, *J. Am. Chem. Soc.* 60 (2) (1938) 309–319, <https://doi.org/10.1021/ja01269a023>.
- [54] T.L. Hill, Statistical mechanics of multimolecular adsorption. I, *J. Chem. Phys.* 14 (4) (1946) 263–267, <https://doi.org/10.1063/1.1724129>.
- [55] L. Marmoret, F. Collet, H. Beji, Moisture adsorption in glass wool products, *High Temp., High Press.* 40 (1) (2011) 31–46.
- [56] M. Jiříčková, R. Černý, Effect of hydrophilic admixtures on moisture and heat transport and storage parameters of mineral wool, *Constr. Build. Mater.* 20 (6) (2006) 425–434, <https://doi.org/10.1016/j.conbuildmat.2005.01.055>.
- [57] R.J. LeVeque, *Finite Volume Methods for Hyperbolic Problems*, *Cambridge Texts in Applied Mathematics*, vol. 31, Cambridge University Press, New York, USA, 2002.
- [58] E. Süli, D.F. Mayers, *An Introduction to Numerical Analysis*, Cambridge University Press, Cambridge, UK, 2003.
- [59] S. Balay, S. Abhyankar, M.F. Adams, S. Benson, J. Brown, P. Brune, K. Buschelman, E.M. Constantinescu, L. Dalcin, A. Dener, V. Eijkhout, J. Faibussovitch, W.D. Gropp, V. Hapla, T. Isaac, P. Jolivet, D. Karpeev, D. Kaushik, M.G. Knepley, F. Kong, S. Kruger, D.A. May, L.C. McInnes, R.T. Mills, L. Mitchell, T. Munson, J.E. Roman, K. Rupp, P. Sanan, J. Sarich, B.F. Smith, S. Zampini, H. Zhang, H. Zhang, J. Zhang, *PETSc Web page*, <https://petsc.org/>, 2023.
- [60] L.D. Dalcin, R.R. Paz, P.A. Kler, A. Cosimo, Parallel distributed computing using Python, *Adv. Water Resour.* 34 (9) (2011) 1124–1139, <https://doi.org/10.1016/j.advwatres.2011.04.013>.
- [61] P. Virtanen, R. Gommers, T.E. Oliphant, M. Haberland, T. Reddy, D. Cournapeau, E. Burovski, P. Peterson, W. Weckesser, J. Bright, S.J. van der Walt, M. Brett, J. Wilson, K.J. Millman, N. Mayorov, A.R.J. Nelson, E. Jones, R. Kern, E. Larson, C.J. Carey, Í. Polat, Y. Feng, E.W. Moore, J. VanderPlas, D. Laxalde, J. Perktold, R. Cimrman, I. Henriksen, E.A. Quintero, C.R. Harris, A.M. Archibald, A.H. Ribeiro, F. Pedregosa, P. van Mulbregt, *SciPy 1.0 contributors*, *SciPy 1.0: fundamental algorithms for scientific computing in Python*, *Nat. Methods* 17 (2020) 261–272, <https://doi.org/10.1038/s41592-019-0686-2>.